Assessing the multidimensional complexity of biodiversity using a globally standardized approach

Authors: Robert M. McElderry[1,2]*, Camille Fournier de Lauriere[1], Charbel El Khoury[1], Priyanka Chaudhary[1], Shivakumara Manu[1], Felix Specker[1], Ian Brettell[1], Johan van den Hoogen[1], Daniel S. Maynard[3], Carolina Bello[1], Lalasia Bialic-Murphy[1], Camille S. Delavaux[1], Daisy H. Dent[1,4,5], Thomas W. Elliott[1,6], Laura G. van Galen[1], Thomas Lauber[1], Andrea Paz[7], Gabriel Smith[1], Leland K. Werden[1], Constantin M. Zohner[1], Thomas W. Crowther[1,6]

Affiliations:

1. Institute of Integrative Biology, ETH Zürich (Swiss Federal Institute of Technology), 8092 Zürich, Switzerland
2. Swiss Federal Institute for Forest, Snow and Landscape Research (WSL), 8903 Birmensdorf, Switzerland
3. Department of Genetics, Evolution, and Environment, University College London, London, UK
4. Smithsonian Tropical Research Institute, Ancon, Panamá, República de Panamá
5. Max Planck Institute of Animal Behavior, Konstanz 78315, Germany
6. Restor Eco AG, 8001 Zürich, Switzerland
7. Départment de Sciences Biologiques, Université de Montréal, Montréal, Québec, Canada

Author list footnotes:

* Correspondence: robert.mcelderry@usys.ethz.ch

Highlights

1. The value of nature lies in its complexity.
2. We define a global framework for a holistic measure of the state of nature.
3. Inclusion of microbes and invertebrates is crucial to evaluate biodiversity.
4. Human activity consistently reduces and homogenizes biodiversity worldwide.

Summary

Quantifying biodiversity across the globe is critical for transparent reporting and assessment under the Kunming-Montreal Global Biodiversity Framework. Understanding the complexity of biodiversity requires consideration of the variation of life across genes, species, and ecosystems. Achieving this in a standardized way remains a key challenge for creating an equitable nature positive future. Here, we present the Sustainable Ecology and Economic Development (SEED) framework, which assesses the dimensions that structure biodiversity patterns worldwide (genetics, species, and ecosystems) across plants, animals, and microbial taxa, and consolidates this into a single measure of biocomplexity at every location, relative to a ‘reference’ ecosystem with minimal human disturbance. We describe the SEED methodology and highlight its features, which include seven novel measures of biodiversity intactness that are integrated into the SEED biocomplexity index. SEED will continuously integrate new datasets and maps to provide up-to-date estimates of local biocomplexity across the planet, providing a tool for decision makers to assess and improve the global state of nature.

Keywords

Biocomplexity; biodiversity monitoring; biodiversity intactness; genetic diversity; species diversity; ecosystem diversity

Abbreviations

SEED	Sustainable Ecology and Economic Development
GBF	Kunming-Montreal Global Biodiversity Framework
GEO BON	Group on Earth Observations Biodiversity Observation Network
EBV	Essential Biodiversity Variable
IUCN	International Union for Conservation of Nature
EII	Ecosystem Integrity Index
BII	Biodiversity Intactness Index
MSA	Mean Species Abundance
HMI	Human Modification Index
PNV	Potential Natural Vegetation

1. Introduction

Every species depends on other species to survive. This vast interdependence means biological diversity is critical for the maintenance of life as we know it. However, humans have historically valued the components of nature we can use for food, timber, and medicine over others[1,2]. The development of markets for these products has incentivized their mass propagation at the expense of other components of biodiversity, driving the oversimplification of biological systems and the loss of the ecosystem services on which we depend[3].

As nature positive policy frameworks and nature markets emerge, it is critical that we learn from past challenges. Mechanisms that value a single aspect of nature – such as carbon sequestration – risk driving the oversimplification of the system[4–7]. This can lead to potentially counterproductive outcomes, like the creation of monocultures of exotic tree species at the expense of local biodiversity[7] and human wellbeing[8]. If political and financial structures are to promote the conservation of natural biodiversity, they must be underpinned by robust scientific monitoring that reflects the full dimensionality of life, across genetic, species and ecosystem levels.

The most prominent guidelines for biodiversity monitoring are described within the Kunming-Montreal Global Biodiversity Framework (GBF)[9], which sets a series of global targets to halt and reverse nature loss by 2030. Key targets in the GBF include protecting areas of high biodiversity importance (Target 1), restoring 30% of degraded areas by 2030 (Target 2), and the headline ‘30x30’ target that aims to conserve 30% of the Earth’s surface by 2030 (Target 3). In the financial sector, the GBF requires businesses to disclose their impacts on biodiversity (Target 15), and the Taskforce on Nature-related Financial Disclosures was assembled to provide guidance and outline best practices for nature-related disclosures. At the heart of nature-related disclosures is a measure of the “state of nature” against which impacts, dependencies, risks, and opportunities may be measured[10]. However, it is not well defined what constitutes a suitable measure of the state of nature.

A growing number of metrics have been developed to measure and monitor biodiversity. Biodiversity metrics generally fall into two categories based on their dataset and scope: local ground-sourced data (e.g. plot surveys, eDNA, bioacoustics monitors and camera traps), and global remotely-sensed data (e.g. radar and multispectral imagery from satellites)[11]. While ground-sourced data are critical for providing detailed insights into the diversity of organisms in a specific study area, their insights may be limited outside the local study sites[12,13]. By contrast, remotely-sensed data can provide globally-standardized assessments of ecosystem-scale characteristics like forest structure[14] and connectivity[15], but not all aspects of nature can be measured directly from satellites. Many global biodiversity metrics incorporate both ground-sourced and remote-sensed data to offer a balance between local relevance and global scope. To align monitoring efforts, the Group on Earth Observations Biodiversity Observation Network (GEO BON) recently proposed a worldwide system of observation networks[16] and established guidelines for 16 Essential Biodiversity Variables (EBVs)[17,18]. However, we lack a coherent method to consolidate these EBVs and all other biodiversity metrics for a unified evaluation of nature.

To address the need for a unified, globally standardized measure of biodiversity across all taxa and scales of variation, we first review existing global biodiversity metrics and highlight their strengths and weaknesses in measuring the current state of nature (Section 2). We then present a new integrative framework, the Sustainable Ecology and Economic Development (SEED), which is designed to consolidate three primary hierarchical levels that underpin biodiversity – genetic, species, and ecosystem – into a global measure of biocomplexity (Section 3). Nature is inherently complex, and biocomplexity is defined as the emergent properties from multiple, often hierarchical levels of interacting factors that "affect, sustain, or are modified by living organisms, including humans"[19]. Recognizing this complexity, we designed SEED so that it can integrate numerous global biodiversity maps and include new maps as they become available. This ensures that policy and market tools will have the most up-to-date information on the state of nature.

2. Current state of global biodiversity measurement

Spatially-explicit biodiversity data products consist of a heterogeneous mix of calculations, model predictions, metrics (standard of measure), and indices (aggregation of multiple indicators). Given our exclusive focus on data products mapped over the globe, we hereafter refer to these products in general as 'maps'. We grouped existing maps into three main organizational levels of ecological systems: within-species genetic diversity, among-species diversity, and ecosystem diversity. Global maps at each level reflect different dimensions of diversity that are essential for a holistic understanding of biocomplexity across the globe. Although some global maps correspond to a given EBV[20], the EBVs do not consist of a set of spatially-explicit global maps[21]. Their main purpose is to identify the key variables and provide standards on how to measure them[17]. Rather than discuss this detail in depth, we identify the strengths and weaknesses of existing maps and the considerations for including them in a unified measure of biodiversity. We conclude this section with a brief description of a fourth group of maps that represent standardized measures of biodiversity.

2.1 Genetic (within-species) diversity

Genetic diversity (heritable variation) represents variation in the genetic composition of individuals within a species and among populations and is the source for adaptive responses to environmental change[22,23]. There are few global measures of genetic diversity and these are estimated from mitochondrial DNA sequences stored in the National Centre for Biotechnology Information GenBank and the Barcode of Life Database[24–26]. While there are good insights about genetic variation for certain plant[27] and animal species[24–26], we currently lack global predictions of genetic variation for most species on the planet. Among the few taxonomic groups that have been studied, loss of genetic diversity is often correlated with the loss of suitable habitat[28] and reduced abundance[29]. This may suggest that we could use measures of population declines to generate proxy measures of decline in genetic diversity, but this population timeseries data is lacking for the vast majority of organismal groups, except for the 5,200+ species in the Living Planet Database[30]. However, with modern advancements in genetic sequencing technology and widespread usage of barcoding and metabarcoding[31], new data are continually becoming available that will enable the global measurement of genetic diversity across taxonomic groups[23].

2.2 Species, phylogenetic, and functional diversity

Traditionally, global biodiversity research has primarily focused on species richness (the number of unique taxa). However, species diversity also includes phylogenetic (i.e., a measure of evolutionary history[32]) and functional diversity, and adding these dimensions adds depth to our description of natural communities. Species richness maps are generally created by overlaying several species range maps then summing the number of species per pixel[33–35], which in some models is then modeled against a set of predictor variables before predicting richness[36–38]. Phylogenetic and functional diversity are calculated using a phylogeny[39] or a functional-trait matrix[40] to quantify the unique contributions from each of the species present at each locality and thus provide information about phylogenetic and functional components of diversity. Whereas a species-rich community may be composed of evolutionarily and functionally redundant species, other less species-rich communities may (or may not) have more evolutionarily and functionally divergent species that may contribute unique functions to the community. Therefore, highlighting those communities with particularly rich evolutionary roots and functional traits is key for a holistic measure of biodiversity.

Species diversity maps inherit biases from their underlying data sources that may affect their applicability. All global biodiversity databases over-represent some regions and under-represent other regions, typically with a bias toward developed nations[41], and there are considerable disparities in taxonomic coverage, with a bias toward larger and more charismatic organisms. The IUCN database – the source of many biodiversity maps[24,25,42–45] – contains distribution data for over 80% of described vertebrate species and 14% of vascular plants, but only 2% of invertebrate species, which represent the vast majority of animal species diversity. In addition, microbes represent 88% to 99% of all species on Earth[46,47] but are vastly underrepresented, with only 0.4% of known fungi and protists included in the IUCN database. This pattern is now changing due to recent advances in high-throughput sequencing technologies that enable us to observe and quantify microscopic and otherwise cryptic species[48], and the availability of microbial biodiversity maps is expanding exponentially[49–52].

Species diversity maps are also limited by their original scope and the underlying models. Until now, most global maps of species diversity were not designed to capture fine-scale patterns in species composition, or the effects of local human disturbance. With a focus on broad-scale biogeographic trends, species diversity models focus climate, edaphic and topographic predictive variables to predict diversity patterns across environmental gradients. The general lack of human influences in these models leads to low predictive accuracy for quantifying the impacts of human disturbance (Figure 1). This may be due in part to the recent emergence of global human modification maps[53–56] and also due to a paucity of biodiversity data in both heavily degraded and intact landscapes. Furthermore, species diversity maps tend to be temporally static, calculated as an average of observations that can span decades. Additionally, sampling methodologies are taxon and/or habitat specific and may also differ by region and discipline or agency. These complexities make it difficult to harmonize available data and generate well-rounded estimates that scale in space and change over time in response to shifting conditions on the ground.

2.3 Ecosystem diversity

In contrast to genetic and species diversity, which rely heavily on ground-sourced data, ecosystem-level maps provide a more up-to-date view of current conditions because they can be measured directly from satellite imagery, or modeled based on spectral imagery (e.g., radar and multispectral imaging). A wealth of global-scale remote sensing products have been designed to capture information about human modifications[55], land use change[57], canopy cover[58], canopy height[59], above and belowground biomass[60,61], soil respiration[62], habitat heterogeneity[63], leaf area index[64], ecosystem connectivity[65,66], net primary productivity[67] and ecological resilience[68,69]. We group all ecosystem-level maps that measure some aspect of biodiversity into one of three broad categories: ecosystem structure, function[17], or connectivity.

Ecosystem structure, function, and connectivity are emergent properties that arise from the combination of species, landscape physiognomy, climate, and human modifications. For example, the occurrence and extent of mangroves[70] and peatlands[71,72] are due to relatively specific sets of conditions, and their structural features are critical to their functional roles. The interplay between living organisms and their environment are also key ecosystem properties, perhaps best exemplified by plant-disperser and plant-fungal associations. Global maps of plant-disperser associations or species interaction networks are not currently available, but progress in this field indicates potential for such maps in the future[73]. The field of plant-fungal associations has produced numerous global maps, which predict such functional features as the relative proportions of nitrogen fixing and arbuscular mycorrhizal or ectomycorrhizal associated plants[74] and the densities of their fine roots[75] over the landscape, which may affect the intensity of mycorrhizal colonization[75], soil moisture[76] and decomposition rates[77]. These ecosystem properties provide a direct link to measures of ecosystem services[78,79]. Just as the three-dimensional structure of an ecosystem characterizes the environmental context in which species coexist, the spatial arrangement of habitat fragments and species-specific dispersal abilities and limitations determine ecosystem connectivity. Ecosystem connectivity tends to decrease with habitat loss and fragmentation, and both connectivity[80] and fragmentation[81] indices can provide unique insights into the ecological functionality at the landscape-scale[82].

2.4 Standardized measures of biodiversity

Given the challenges of capturing dynamic changes in ecological diversity at a global scale, a few analyses estimate how far the ecological community has diverged from its natural state. Using a database from targeted experiments and local studies spanning disturbance gradients, it is possible to identify how land use change affects ecological diversity and use these relationships to predict ecological intactness across the globe. Three commonly used global indices are the Ecosystem Integrity Index (EII)[83] by the United Nations Environment Programme World Conservation Monitoring Centre, the Biodiversity Intactness Index (BII)[84,85] by the Natural History Museum in London, and the Mean Species Abundance (MSA)[86] index by the Netherlands Environmental Assessment Agency.

The EII includes three components: structure, function, and composition. Ecosystem structure is based on the human modification index (HMI)[55]; ecosystem function is measured by the ratio of actual to potential net primary productivity[67]; and ecosystem composition is measured by the BII[84,87]. For a given location, the EII uses the lowest score of the three components to predict the extent to which any ecosystem has been impacted or altered from its original state. The BII uses a linear model of the impacts of land use and related pressures on two aspects of biodiversity, species abundances and compositional similarity, to estimate the intactness of a community of plants, vertebrates, and invertebrates. The MSA index is conceptually similar to the BII but focuses mainly on species abundance, includes additional human-related pressures, and estimates an average intactness value that is weighted by the land use type and its associated human pressures.

The MSA, BII, and EII represent the current state-of-the-art in global biodiversity modeling. Yet, there are two key aspects of diversity that these indices do not capture. First, these indices are fairly limited in taxonomic scope. The BII and EII (and to some degree MSA) are primarily based on the PREDICTS database (Projecting Responses of Ecological Diversity In Changing Terrestrial

Systems)[88], which is valuable for quantifying the impact of land use on biodiversity in different regions of the globe. However, at present, the data coverage of PREDICTS represents a relatively limited taxonomic range, including less than 10% of the described species for most large taxonomic groups like vascular plants and invertebrate animals, and a far smaller proportion for microbes[88,89]. Given that these taxa respond differently to human disturbance and show unique global distribution patterns[90,91], the underrepresentation of important taxa may therefore bias global biodiversity assessments. Second, these indices focus exclusively on species level diversity and do not include genetic diversity or, except for the EII, ecosystem level properties that emerge from the web of interactions among species and their environment.

3. A framework for observing biological complexity on Earth

With the increasing combination of ground-sourced and remotely-sensed data, we are at the beginning of a data revolution in global ecology[92,93]. The exponential growth of global ecological datasets and maps across genetic, species, and ecosystem levels represents exciting new opportunities for our understanding of biodiversity across the planet. Conceptual frameworks that integrate and interpret this growing body of information are essential to generate a holistic understanding of global biocomplexity. Our global understanding of biocomplexity will never be fully complete, as emerging scientific assessments continue to capture novel information. Therefore, it is important to establish flexible and dynamic frameworks that can incorporate new and emerging information as it becomes available.

A key element in new nature-related disclosure frameworks is a vaguely defined measure of the state of nature[10], which would presumably represent the full multidimensional complexity of nature, but for which there is currently no agreed upon metric. To address the need for a unified state of nature metric, we present a holistic ecological framework (hereafter referred to as SEED) that is designed to represent the multidimensionality of nature by defining nine axes of variation, nested within the three hierarchical levels of diversity: genetics, species (including phylogenetic and functional diversity), and ecosystems (Figure 2). Within the genetic and species levels of variation, we include plants, animals, and microbes. The grouping of microbes to include archaea, bacteria, protists, and fungi could be disaggregated in the future as more information becomes available. Within ecosystems, we distinguish three axes: structure, function, and connectivity. The SEED framework incorporates all existing biodiversity maps and will update frequently to include the best available information. The SEED framework incorporates components already identified as EBVs by GEO BON[17] (Figure 2) and generates summary indices for the nine axes of biodiversity alongside a unified biocomplexity index. We apply the term biocomplexity[19] to set it apart from measures of single biodiversity components, and to highlight the inclusion of multiple hierarchical levels of diversity, which emerge not just from the complex interplay between biological life and the environment, but also from the billions of years of physical and biological evolution on Earth.

To globally-standardize the biocomplexity index, we estimate the similarity (ranging from zero and one) between the current state of an ecosystem and its natural state, which we measure over a suite of biodiversity maps in reference areas that we identify using the Human Modification Index to have only experienced minimal human disturbance (see Section 3.2). The SEED framework first summarizes the intactness (i.e., similarity to natural state) of multiple underlying biodiversity features in each axis, which allows each axis to be viewed separately to aid comprehension and facilitate action-impact assessments. We summarized this information a radar plot (Figure 2), whereby the intactness values for each axis at a site are plotted on scale from zero to one. The SEED framework also calculates the mean intactness for all nine axes combined to create a unified score: the SEED biocomplexity index, which also ranges between zero and one, where values near zero represents the near absence of biocomplexity (e.g., an open pit mine or paved area), and one represents an area that is equal to its potential natural state (i.e., a minimally-disturbed ecosystem). The SEED framework therefore offers both a single standardized biocomplexity value for any area of interest and nine intactness indices for each axis of biodiversity, thus allowing the user to unpack this information.

3.1 Integrating dimensions of biodiversity

Consolidating the multiple hierarchical levels of biodiversity into a single value is a critical feature that makes our biocomplexity index generalizable and comprehensible. All available global maps are combined within each of the relevant biodiversity axes (Figure 2), using a multivariate kernel estimator[94] (Eq. 1), and then the mean of these nine axes consolidates this information into a single biocomplexity index.

$$K(\boldsymbol{z}, \boldsymbol{z}_r) = exp[-\delta \|\boldsymbol{w} \circ (\boldsymbol{z} - \boldsymbol{z}_r)\|_1] \quad \text{(Eq. 1)}$$

Here, $\boldsymbol{z}$ is a n-dimensional data vector for a given location, where n represents the number of input maps involved in the calculation. The term $\|\boldsymbol{w}(\boldsymbol{z} - \boldsymbol{z}_r)\|_1$, represents the Manhattan distance, (or ℓ^1 distance), between the data vector $\boldsymbol{z}$ and the mean values for the corresponding reference areas $\boldsymbol{z_r}$ after elementwise multiplication ($\circ$) by the n-dimensional vector, $\boldsymbol{w}$, which contains the normalized weight for each input map. The resulting distance value is then converted into a similarity value, which is bounded by zero and one, by applying the kernel function, K, where δ represents a scaling parameter.

Sensitivity of similarity is set by the scaling parameter, δ, which we set for each biodiversity axis according to two criteria. First, δ must be strictly positive to ensure that the kernel values are bound between zero and one. Second, the similarity values measured by K capture the intactness of nature and should span the full range between zero and one. We set δ to the lowest value that met these criteria, given that increasing values simply shifted the distribution further to the left toward zero intactness (see Supplement S1).

The weight of information is the final key consideration in our kernel estimator. We designed this framework to integrate numerous biodiversity maps, and we test it here with 75 maps (Table S2) – ecosystem structure (25), function (12), and connectivity (1); species diversity of plants (11), microbes (13), and animals (11); and genetic diversity of animals (2). We reprojected all maps to a common projection (epsg:4326) and spatial resolution (30 arc-seconds, ~926 meters at the equator) using a nearest-neighbor algorithm. The maps we reviewed vary in several aspects: coverage extent, spatial resolution, non-independence from other maps, extrapolation across regional data gaps, and in the degree to which satellite imagery or other measures of local conditions were integrated. We developed a dynamic weighting system to define the normalized weight of each map in a set, represented by $\boldsymbol{w}$. We grouped non independent layers to share equal weight, which resulted in a short hierarchical structure. We also applied a confidence score and associated decreasing confidence with decreasing weight (see Supplement Table S1 for details). Although we found no global maps of the genetic diversity of plants or microbes, we filled in two blank maps to test the full framework and set the weight of these maps to a very small nonzero number.

We structured the integration of the nine biodiversity axes to be an even-weighted average of the intactness in each dimension. This places genetic, species, and ecosystem level diversity on equal grounds in the integrated index. SEED also offers an index for each biodiversity axis for independent use alongside the integrated index. Even weighting ensures equitability within genetic and species diversity among plants, animals, and microbes, which deviates strongly from the more common case wherein smaller, more cryptic taxa are overlooked in favor of more visible or personable taxa. If, however, evidence emerges that suggests a different weighting scheme is warranted, our method can be adapted in accordance with the evolving scientific landscape. In practice, however, the availability and quality of available maps is not even among axes, which resulted in some axes having higher relative weight and therefore more influence on the overall biocomplexity index (See Supplement S1 for details on how confidence scores affect the relative weights among axes). Identifying the optimal weighting for various levels of biodiversity information remains a key challenge for future biodiversity research as our theoretical understanding of ecological systems evolves.

3.2. Reference area versus a counterfactual landscape

To measure the intactness of biocomplexity requires establishing a baseline potential state that can be used for comparison. Estimating this baseline state poses several philosophical questions regarding the non-static nature of natural systems. It also poses data limitations for regions of the world that have been heavily degraded and thus lack ‘pristine’ potential states, such as large regions of the Northern Hemisphere[95]. Thus, we opt for a more direct approach than estimating a potential natural state for all biodiversity axes and underlying layers. We identify minimally-modified areas as points of reference with a procedure that involves few assumptions, considers the full suite of biodiversity together, and allows for a contemporary definition of natural as opposed to a historical estimate[96].

Specifically, we developed an algorithm that uses the HMI[55] and potential natural vegetation (PNV)[57] to select reference areas for each land cover class within each of the 846 ecoregions[97] on Earth. This was done separately for each ecoregion to ensure ecologically relevant comparisons. In each ecoregion, we identify the least impacted areas for each land cover class (from the PNV), using a dynamically-defined, upper-limit HMI threshold to ensure a sufficiently large area, enabling representative and robust estimates (see Figure 3a and Supplement S1). The mean value for each biodiversity feature layer within this *least-impacted area* estimates $\boldsymbol{z_r}$ in equation 1 and is the basis for comparing all feature values in all pixels of the same vegetation class within that ecoregion.

Although a natural landscape with minimal anthropogenic disturbance is not a universal goal in all scenarios, this minimal-disturbance baseline provides an objective, and replicable benchmark for measuring the state of nature. For example, food security and financial wellbeing are the primary considerations in agricultural settings, while restoration targets in conservation settings may deviate from a fully natural state due to a myriad of ecological and socioeconomic factors and needs, as well as previous alterations to the landscape[98]. Management practices and targets will vary depending on the local situation, and progress toward these targets can be evaluated against local minimal-disturbance benchmarks and other landscapes in similar settings. In these contexts, the SEED index provides a useful tool to benchmark local achievement against a globally-standardized biodiversity metric and enables a standardized assessment of biodiversity improvement in response to management practices[17].

3.3. Illustration of the SEED biocomplexity framework

The biocomplexity index was developed using a comprehensive list of the most up-to-date maps of genetic, species, and ecosystem diversity (see Supplement Table S2). Although, our framework is designed to integrate nine biodiversity axes, the current lack of global maps to represent the genetic diversity of plants and microbes limits the current index to seven functioning axes. To illustrate the capabilities of the framework, we first show the viability of our dimensionality reduction calculation (equation 1) and reference area (Figure 3a) approach to calculate the intactness of seven biodiversity axes (Figure 3b-h). Combined, these intactness layers generate a unified measure of the intactness of nature, the SEED biocomplexity index (Figure 4a). We show how SEED can be aggregated across ecological boundaries and at various spatial scales to summarize biocomplexity in total and along each biodiversity axis (Figure 4b-c). Finally, we conduct a cursory comparison of SEED against the leading biodiversity intactness indices (Figure 5).

Among the seven biodiversity intactness indices that we calculated, we identified broad global patterns where the indices unanimously show similar levels of intactness (Figure 3). High intactness is nearly universally indicated across tundra, northern boreal forests, deserts, and the Amazon basin – areas that have not experienced extensive human development. Low intactness is indicated in the temperate grasslands and savannas of North America, Brazil's Atlantic Forest, narrow bands along the West African coast and Sub-Saharan Africa, temperate forests across Europe and east across Asia toward Siberia, Northern India, the western edge of Southeast Asia, Northeastern China, and the eastern and southwestern coasts of Australia.

There is also notable divergence among these indices. While the intactness of plant and microbial species were very similar (Figure 3f-g), and to some degree aligned with ecosystem structure (Figure 3b), ecosystem function (Figure 3d) shows divergent patterns in some regions, e.g., central North America, Western Ghats, and Central Deccan Plateau. Ecologically, we know very well that plants and microbes share special linkages and that ecosystem structure and function result from the local communities of plants, microbes, and animals. The intactness of animal species diversity (Figure 3h) is also divergent and highlights that the Andes and Appalachian Mountain ranges have particularly low intactness of animal species diversity relative to the other indices in these regions. In the Indo-Gangetic Plains, animal species intactness remains relatively high while other indices predict low intactness. Ecosystem connectivity (Figure 3c) shows a largely unique pattern. Currently the SEED connectivity index is highly sensitive to fragmentation[81], and therefore scores land area as either highly intact or not at all. The genetic diversity of animals (Figure 3e) also shows a unique pattern, but this is likely because we have only two genetic diversity maps with very coarse resolution (~380-km)[25]. This along with the absence of global models for plant and microbial genetic diversity emphasizes the need for more work in global modeling of genetic diversity.

The value in our biocomplexity framework is twofold; it integrates information regarding multiple hierarchical levels of diversity and numerous maps within each level, and it can be aggregated to provide summary statistics at the desired scale. The integrated SEED biocomplexity index represents a single measure of the state of nature for terrestrial land area across the globe (Figure 4a). This shows that, on average, the Earth is currently at 68% of its natural state (Figure 4b). Aggregating by administrative boundaries[99], we can evaluate the state of nature at a level where local policies may directly affect the mechanisms governing the direct human impacts on nature (Figure 4c).

In comparison to existing global biodiversity indices, SEED (Figure 4) offers a more comprehensive view of nature's state due to its inclusion of 75 global biodiversity maps, while also offering disaggregated information in the form of seven intactness sub-indices (Figure 3b-h). Existing global intactness indices (BII, and MSA) exclusively represent species level diversity for a subset of taxa. SEED expands the taxa represented with a wealth of microbial datasets (including fungi, bacteria, and archaea), while also expanding in scope to include multiple ecosystem attributes that capture landscape dynamics and ecological feedback. Their inclusion in SEED may account for differences between SEED and the other intactness indices (Figure S1). For example, SEED may indicate low ecosystem intactness where satellite imagery detects ecosystem fragmentation, while models predicting species composition may not register a change in species intactness. Given the global coverage and high temporal resolution of satellite imagery, the inclusion of remote-sensed ecosystem characteristics not only adds dimensionality to biodiversity estimates, but it also improves the spatial and temporal resolution of biodiversity intactness predictions.

3.4. Spatial and temporal scalability and next steps

There is a growing demand for spatial and temporal scalability in global biodiversity monitoring, but achieving this remains a central challenge for ecology. Determining how biodiversity scales in space and time has been the focus of countless investigations, and one general result is that outcomes are highly context-dependent. Meeting the demand for scalability will require reimagining our approach to biodiversity modeling. Work by Map of Life[100] in association with GEO BON exemplifies the scalable biodiversity models of the future. Map of Life provides a catalog of species distributions predicted over space and time, generated using the most up-to-date remote sensing technologies and species distribution models[20]. Bringing these maps together, we can reevaluate species richness, phylogenetic and functional diversity, and genetic diversity via declines in species ranges; and we can generate time series for these biodiversity metrics in high spatial resolution. As these new products emerge, they will be fed directly into the SEED framework to update the biocomplexity index and improve the spatial and temporal resolution of the index to allow for more fine-scale assessments of biodiversity and dynamic changes over time.

The integration of remote sensing in biodiversity modeling will be the key distinguishing factor that transforms novel approaches from simply predicting general patterns to the prediction of local conditions and the actual state of nature. Overall, we gain more complete spatial coverage from remote sensing than would be possible from field observation, with more reliable information than extrapolation of models[101]. Remote sensing can provide the means for both direct – many trees and large animals are visible from space – and indirect biodiversity monitoring via the coupling of remote sensing products with ecological models[102]. Future advances in remote sensing such as hyper-spectral imaging[103,104] are expected to provide valuable additional information, which may help assess how plant species and functional biodiversity respond to different practices[105].

Global biodiversity monitoring undoubtedly requires a combination of ground-sourced and remote-sensed approaches. Future on-the-ground sampling in under-sampled regions of the planet and for under-sampled taxa like invertebrates is urgently needed to fill in key gaps and narrow the uncertainty in global genetic and species diversity models. The emergence of next-generation technologies – such as eDNA[48,106], bioacoustics[107], and camera traps – may prove to be essential for scaling data collection in a cost-effective manner[108]. Incorporation of these emerging technologies is a core aim in the continual development and fine-tuning of the SEED framework to ensure the best possible estimation of biodiversity.

4. Conclusion and outlook

There is growing recognition that we need both the political will and mechanisms to distribute finance towards local efforts that promote biodiversity[109]. To support this transition to equitable biodiversity protection, we require globally standardized assessments of ecological intactness that can detect change over time and are available to everyone, everywhere. Given the expansion of global datasets reflecting various dimensions of biodiversity across plants, animals, and microbes, frameworks for integrating this information are now within our grasp. The resulting global assessments of biocomplexity are necessary to evaluate progress toward climate change and land protection pledges (e.g. the GBF, Bonn Challenge[110], and UN Sustainable Development Goals[111]), bring transparency to policy frameworks, and to encourage corporate accountability (under the Taskforce for Nature-related Financial Disclosures (TNFD)[10] and Science-Based Targets for Nature (SBTN)[112]).

The SEED framework consolidates the three primary levels of biodiversity to produce a standardized and comprehensible measure of biocomplexity across the globe. This framework is fundamentally collaborative, incorporating biodiversity assessments and models from a diverse range of biodiversity experts. In addition, it is flexible, allowing for a dynamic index that evolves alongside the development of new map products and scientific advancements. We demonstrate that the SEED framework captures multidimensional changes in biodiversity along seven distinct axes (Figures 3) and provides a unified understanding of the state of nature at multiple scales (Figure 4). Yet, there are several key challenges that need to be addressed to improve the resolution of our index at finer spatial and temporal scales. Most notably, the development of models that integrate remote sensing data products into maps of species richness and genetic diversity will greatly improve the spatial and temporal resolution of our index.

To ensure that the most high-integrity and up-to-date ecological information is available to policy- and decision-makers, we invite the wider scientific community to collaborate on the continual advancement of this biocomplexity index (www.seed-index.com). We believe that for this biodiversity index to lead to positive outcomes, its satellite-based predictions must accurately represent the actual biodiversity at a site. Achieving this level of accuracy presents a scientific challenge that requires the collaboration of a diverse team of experts, including ecologists, remote-sensing specialists, and others from around the globe. Leveraging the latest scientific and technological breakthroughs, we aim to enhance and refine the biocomplexity index, thus fostering better outcomes for ecosystem protection and restoration.

Figures

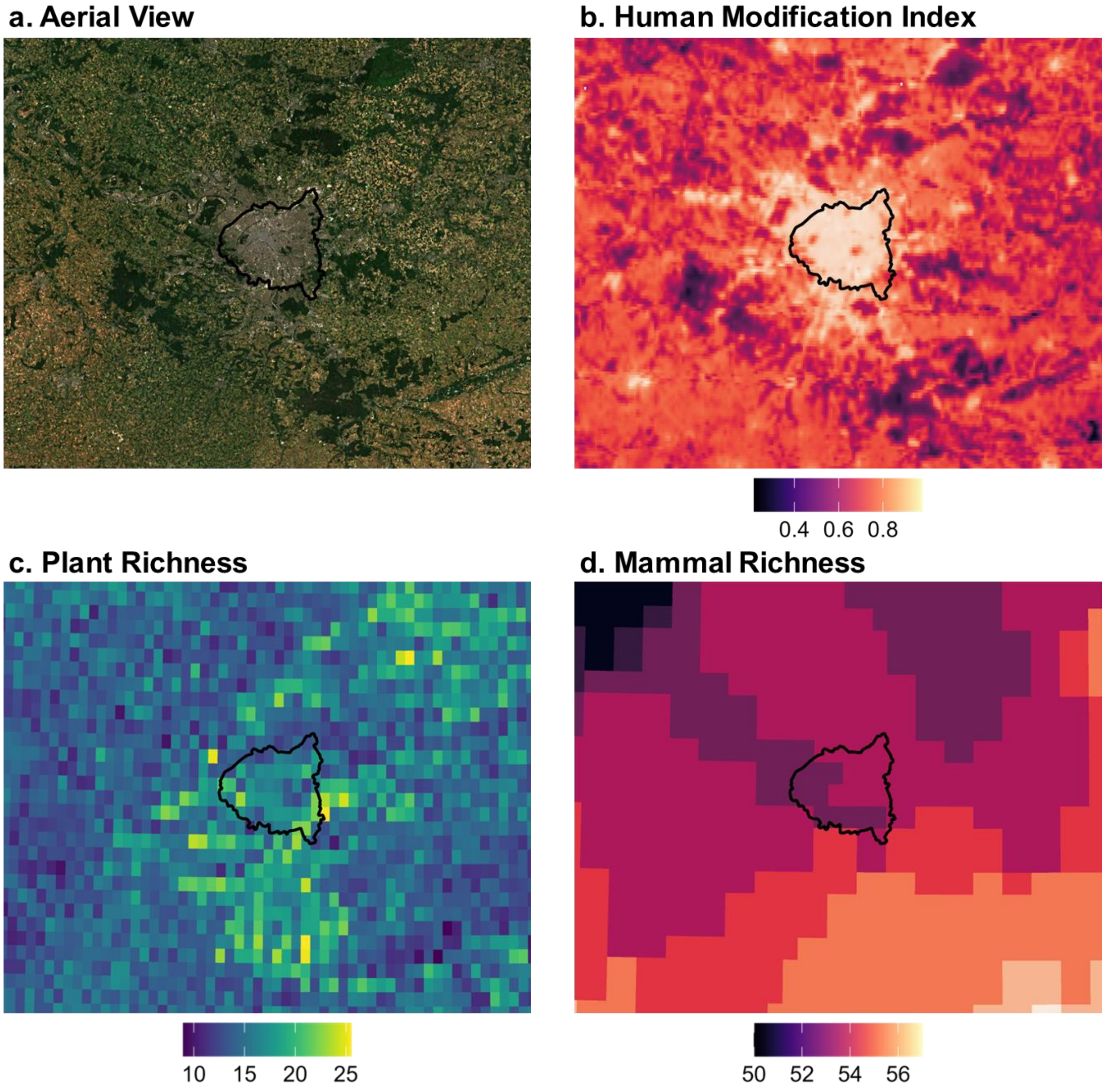

Figure 1. Poor performance of species richness maps in human modified landscapes. The impacts of human activities – as is shown here for Paris (outline) and the surrounding landscape (a) in satellite imagery[113] and (b) in the human modification index[55] – were not included in the development of most maps of species richness, e.g., (c) plant[114] and (d) mammals[34].

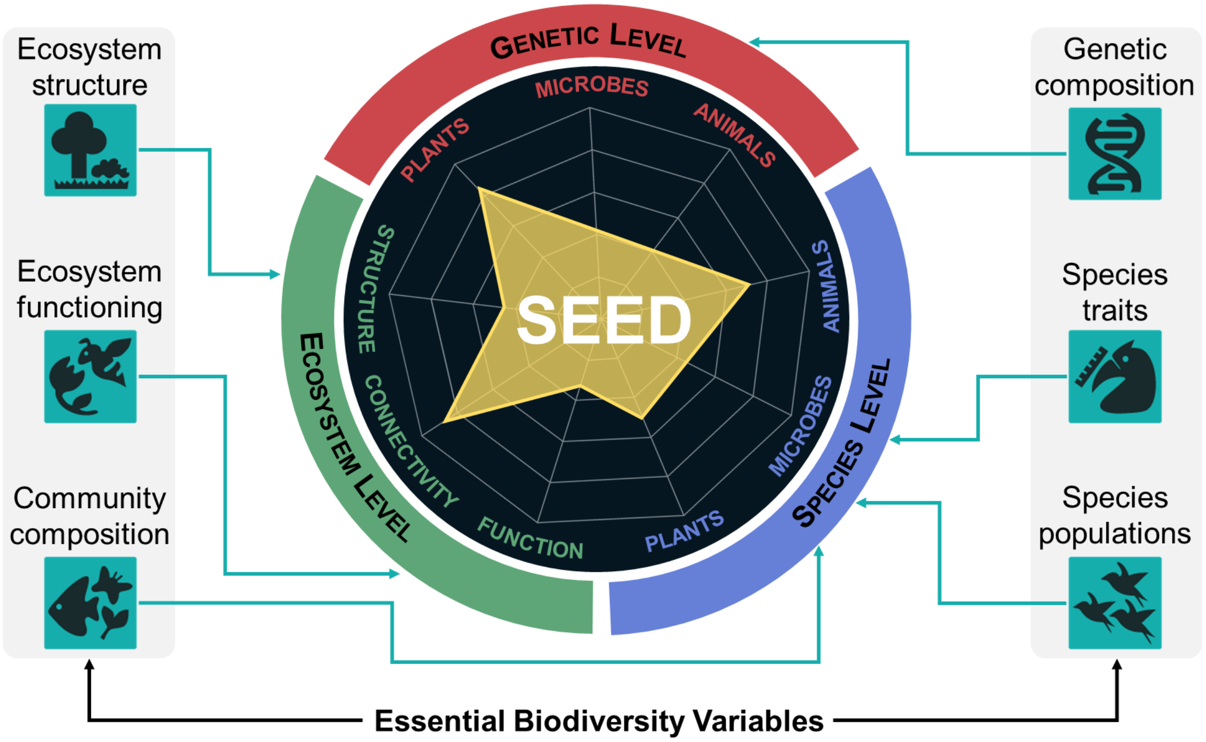

Figure 2. **SEED biocomplexity index.** Example visualization of the SEED framework for an area of interest, showing the dimensionality-reduced intactness scores across the nine dimensions of biodiversity. Along each axis the yellow line measures the intactness, the similarity of the current state and the potential natural state based on a comparable, minimally-disturbed ecosystem. For this area of interest, the average of these values, weighted by the quality of the data, yields the SEED biocomplexity index and indicates the total intactness of nature. Arrows trace the relationships between SEED's biodiversity dimensions and the Essential Biodiversity Variables (EBVs)[17].

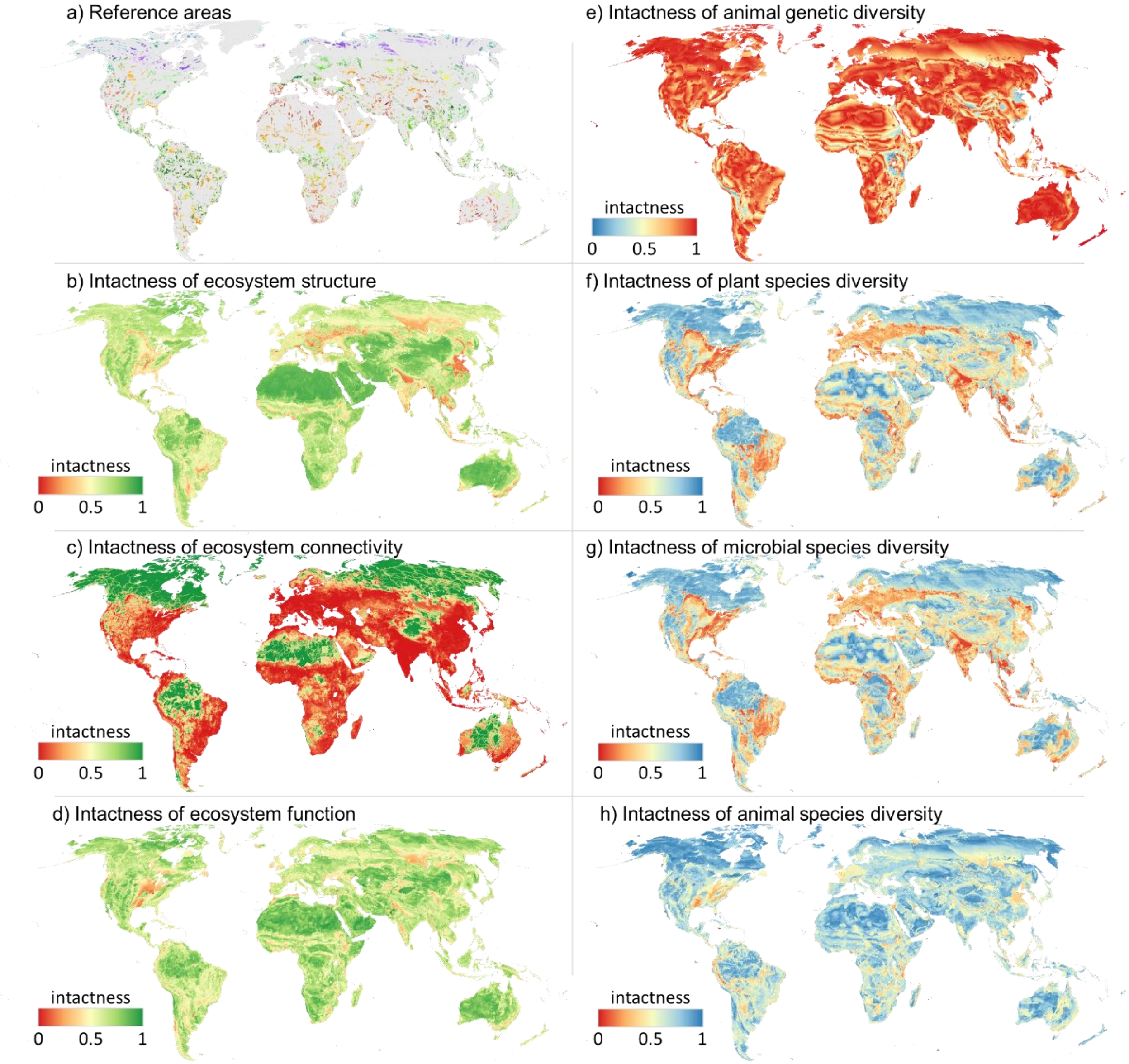

Figure 3. A reference area approach to measuring intactness along seven axes of biodiversity. Series of maps showing the intactness – relative to (a) minimally impacted reference areas (colored by ecoregion[97]) – of diversity along seven biodiversity axes: ecosystem (b) structure, (c) connectivity, and (d) function, genetic diversity of (e) animals, and species diversity of (f) plants, (g) microbes, and (h) animals.

a) SEED biocomplexity index

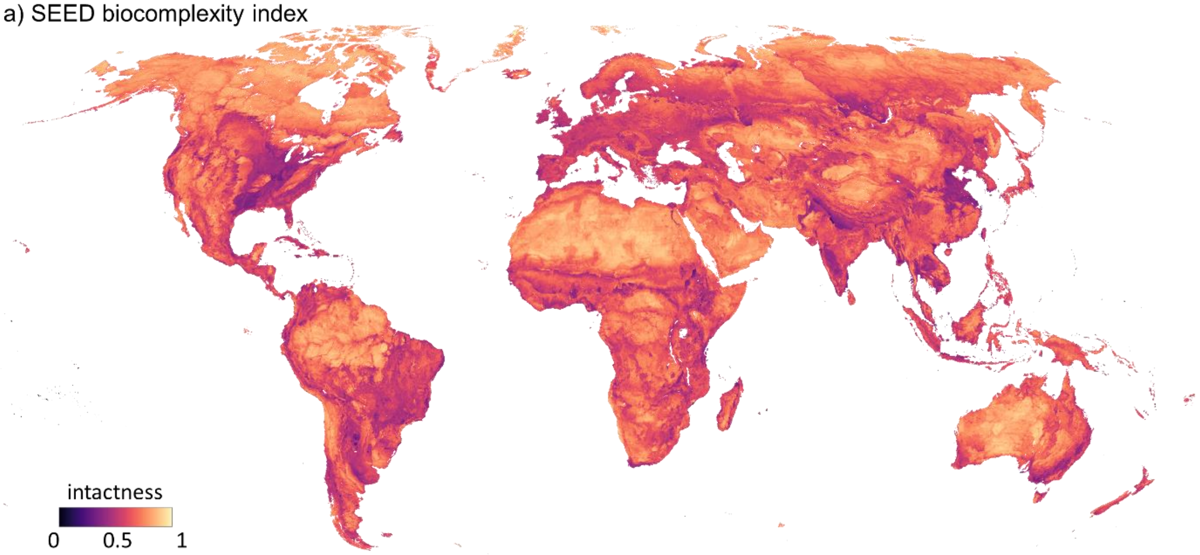

b) Global SEED analysis

c) Mean biocomplexity at administrative level 1

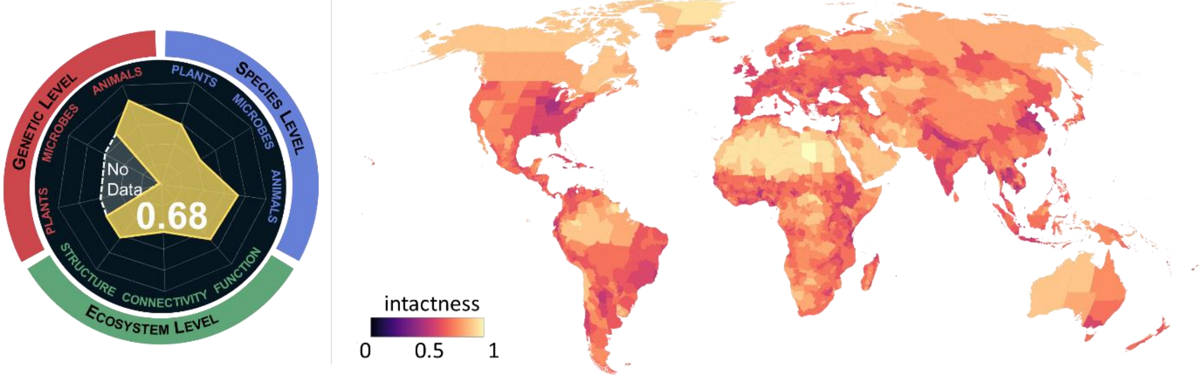

Figure 4. Global analysis of biocomplexity. Map of the (a) SEED biocomplexity index, which measures the intactness of biodiversity for every 1-km of pixel of land. SEED can be aggregated across ecological boundaries, as is demonstrated with (b) a global analysis and (c) the summaries by administrative boundaries.

Resource availability

Lead contact: Requests for further information and resources should be directed to and will be fulfilled by the lead contact, Robert McElderry (robert.mcelderry@usys.ethz.ch).

Materials availability: All unique biodiversity indices generated in this study may be accessed at https://doi.org/10.5281/zenodo.13799961

Data and code availability: This paper analyzes existing, publicly available data. We compiled a list of the sources where these data may be accessed [See Excel file]. All original code is currently unavailable.

Acknowledgements:

This work was supported by DOB Ecology, the Bernina Initiative, and Nestlé. CSD was supported by SNSF Postdoctoral fellowship TMPFP3_209925. DHD and LKW were supported by a Google Carbon Removal Research award. We also thank Jelle P. Hilbers for reviewing our manuscript and offering several useful suggestions.

Author contributions:

This work was conceptualized by TWC, DM, JvdH, TE, RMM, and CFL. RMM, CFL, CEL, FS, PC, TWC, and JvdH developed the methodology while CEL, FS, PC, RMM, TL, CFL, and JvdH composed the software. Data curation, formal analyses, and validation were performed by RMM and CFL with assistance from CEL, SM, PC, JvdH and TL. Resources were curated by TL, CFL, CEL, PC, and RMM. The original draft was composed by TWC, RMM, CFL, and IB, followed by revisions by all authors. Visuals were envisioned by TWC, RMM, and IB, and created by CFL and RMM. TWC and RMM supervised this work, and funding was acquired by TWC, TWE, RMM, LKW, and IB.

Declaration of interests:

Restor (Restor Eco AG) is a non-profit spin-out from the Crowther Lab at ETH Zurich and is wholly owned and financed by the Restor Foundation. None of the authors own any shares in Restor. TWE is the CEO of Restor and TCW is the President of the Council of the Restor Foundation and a member of Restor's Science Advisory Council.

Supplemental information:

Document S1. Additional methods, Table S1, and Figure S1

Table S2. List of layers incorporated in SEED. See Excel file.

Web-based map viewer. https://robertmcelderry.users.earthengine.app/view/seed-biocomplexity-global-beta

6. References:

1. Henle, K., Alard, D., Clitherow, J., Cobb, P., Firbank, L., Kull, T., McCracken, D., Moritz, R.F.A., Niemelä, J., Rebane, M., et al. (2008). Identifying and managing the conflicts between agriculture and biodiversity conservation in Europe–A review. Agric. Ecosyst. Environ. *124*, 60–71. https://doi.org/10.1016/j.agee.2007.09.005.

2. Lécuyer, L., Alard, D., Calla, S., Coolsaet, B., Fickel, T., Heinsoo, K., Henle, K., Herzon, I., Hodgson, I., Quétier, F., et al. (2021). Conflicts between agriculture and biodiversity conservation in Europe: Looking to the future by learning from the past. In Advances in Ecological Research (Elsevier), pp. 3–56. https://doi.org/10.1016/bs.aecr.2021.10.005.

3. Lockwood, J.L., and McKinney, M.L. eds. (2001). Biotic Homogenization (Springer US) https://doi.org/10.1007/978-1-4615-1261-5.

4. Bremer, L.L., and Farley, K.A. (2010). Does plantation forestry restore biodiversity or create green deserts? A synthesis of the effects of land-use transitions on plant species richness. Biodivers. Conserv. *19*, 3893–3915. https://doi.org/10.1007/s10531-010-9936-4.

5. Armenteras, D., Rodríguez, N., and Retana, J. (2015). National and regional relationships of carbon storage and tropical biodiversity. Biol. Conserv. *192*, 378–386. https://doi.org/10.1016/j.biocon.2015.10.014.

6. Lima, T.A., and Vieira, G. (2013). High plant species richness in monospecific tree plantations in the Central Amazon. For. Ecol. Manag. *295*, 77–86. https://doi.org/10.1016/j.foreco.2013.01.006.

7. Barlow, J., Gardner, T.A., Araujo, I.S., Ávila-Pires, T.C., Bonaldo, A.B., Costa, J.E., Esposito, M.C., Ferreira, L.V., Hawes, J., Hernandez, M.I.M., et al. (2007). Quantifying the biodiversity value of tropical primary, secondary, and plantation forests. Proc. Natl. Acad. Sci. *104*, 18555–18560. https://doi.org/10.1073/pnas.0703333104.

8. Hulvey, K.B., Hobbs, R.J., Standish, R.J., Lindenmayer, D.B., Lach, L., and Perring, M.P. (2013). Benefits of tree mixes in carbon plantings. Nat. Clim. Change *3*, 869–874. https://doi.org/10.1038/nclimate1862.

9. Conference of the Parties to the Convention on Biological Diversity (2022). Decision 15/4.

10. TNFD – Taskforce on Nature-related Financial Disclosures TNFD. https://tnfd.global/.

11. Geller, G.N., Halpin, P.N., Helmuth, B., Hestir, E.L., Skidmore, A., Abrams, M.J., Aguirre, N., Blair, M., Botha, E., Colloff, M., et al. (2017). Remote Sensing for Biodiversity. In The GEO Handbook on Biodiversity Observation Networks, M. Walters and R. J. Scholes, eds. (Springer International Publishing), pp. 187–210. https://doi.org/10.1007/978-3-319-27288-7_8.

12. Witmer, G.W. (2005). Wildlife population monitoring: some practical considerations. Wildl. Res. *32*, 259–263. https://doi.org/10.1071/WR04003.

13. Adam, E., Mutanga, O., and Rugege, D. (2010). Multispectral and hyperspectral remote sensing for identification and mapping of wetland vegetation: a review. Wetl. Ecol. Manag. *18*, 281–296. https://doi.org/10.1007/s11273-009-9169-z.

14. LaRue, E.A., Fahey, R.T., Alveshere, B.C., Atkins, J.W., Bhatt, P., Buma, B., Chen, A., Cousins, S., Elliott, J.M., Elmore, A.J., et al. (2023). A theoretical framework for the ecological role of three-dimensional structural diversity. Front. Ecol. Environ. *21*, 4–13. https://doi.org/10.1002/fee.2587.

15. Bishop-Taylor, R., Tulbure, M.G., and Broich, M. (2018). Evaluating static and dynamic landscape connectivity modelling using a 25-year remote sensing time series. Landsc. Ecol. *33*, 625–640. https://doi.org/10.1007/s10980-018-0624-1.

16. Gonzalez, A., Vihervaara, P., Balvanera, P., Bates, A.E., Bayraktarov, E., Bellingham, P.J., Bruder, A., Campbell, J., Catchen, M.D., Cavender-Bares, J., et al. (2023). A global biodiversity observing system to unite monitoring and guide action. Nat. Ecol. Evol., 1–5. https://doi.org/10.1038/s41559-023-02171-0.

17. Pereira, H.M., Ferrier, S., Walters, M., Geller, G.N., Jongman, R.H.G., Scholes, R.J., Bruford, M.W., Brummitt, N., Butchart, S.H.M., Cardoso, A.C., et al. (2013). Essential Biodiversity Variables. Science *339*, 277–278. https://doi.org/10.1126/science.1229931.

18. Walters, M., and Scholes, R.J. eds. (2017). The GEO Handbook on Biodiversity Observation Networks (Springer International Publishing) https://doi.org/10.1007/978-3-319-27288-7.

19. Michener, W.K., Baerwald, T.J., Firth, P., Palmer, M.A., Rosenberger, J.L., Sandlin, E.A., and Zimmerman, H. (2001). Defining and Unraveling Biocomplexity. BioScience *51*, 1018. https://doi.org/10.1641/0006-3568(2001)051[1018:DAUB]2.0.CO;2.

20. Jetz, W., McGeoch, M.A., Guralnick, R., Ferrier, S., Beck, J., Costello, M.J., Fernandez, M., Geller, G.N., Keil, P., Merow, C., et al. (2019). Essential biodiversity variables for mapping and monitoring species populations. Nat. Ecol. Evol. *3*, 539–551. https://doi.org/10.1038/s41559-019-0826-1.

21. Peterson, A.T., and Soberón, J. (2018). Essential biodiversity variables are not global. Biodivers. Conserv. *27*, 1277–1288. https://doi.org/10.1007/s10531-017-1479-5.

22. O'Brien, D., Laikre, L., Hoban, S., Bruford, M.W., Ekblom, R., Fischer, M.C., Hall, J., Hvilsom, C., Hollingsworth, P.M., Kershaw, F., et al. (2022). Bringing together approaches to reporting on within species genetic diversity. J. Appl. Ecol. *59*, 2227–2233. https://doi.org/10.1111/1365-2664.14225.

23. Hoban, S., Archer, F.I., Bertola, L.D., Bragg, J.G., Breed, M.F., Bruford, M.W., Coleman, M.A., Ekblom, R., Funk, W.C., Grueber, C.E., et al. (2022). Global genetic diversity status and trends: towards a suite of Essential Biodiversity Variables (EBVs) for genetic composition. Biol. Rev. *97*, 1511–1538. https://doi.org/10.1111/brv.12852.

24. Miraldo, A., Li, S., Borregaard, M.K., Flórez-Rodríguez, A., Gopalakrishnan, S., Rizvanovic, M., Wang, Z., Rahbek, C., Marske, K.A., and Nogués-Bravo, D. (2016). An Anthropocene map of genetic diversity. Science *353*, 1532–1535. https://doi.org/10.1126/science.aaf4381.

25. Theodoridis, S., Fordham, D.A., Brown, S.C., Li, S., Rahbek, C., and Nogues-Bravo, D. (2020). Evolutionary history and past climate change shape the distribution of genetic diversity in terrestrial mammals. Nat. Commun. *11*, 2557. https://doi.org/10.1038/s41467-020-16449-5.

26. French, C.M., Bertola, L.D., Carnaval, A.C., Economo, E.P., Kass, J.M., Lohman, D.J., Marske, K.A., Meier, R., Overcast, I., Rominger, A.J., et al. (2023). Global determinants of insect mitochondrial genetic diversity. Nat. Commun. *14*, 5276. https://doi.org/10.1038/s41467-023-40936-0.

27. Wesse, C., Welk, E., Hurka, H., and Neuffer, B. (2021). Geographical pattern of genetic diversity in Capsella bursa-pastoris (Brassicaceae)—A global perspective. Ecol. Evol. *11*, 199–213. https://doi.org/10.1002/ece3.7010.

28. Exposito-Alonso, M., Booker, T.R., Czech, L., Gillespie, L., Hateley, S., Kyriazis, C.C., Lang, P.L.M., Leventhal, L., Nogues-Bravo, D., Pagowski, V., et al. (2022). Genetic diversity loss in the Anthropocene. Science *377*, 1431–1435. https://doi.org/10.1126/science.abn5642.

29. Canteri, E., Fordham, D.A., Li, S., Hosner, P.A., Rahbek, C., and Nogués-Bravo, D. (2021). IUCN Red List protects avian genetic diversity. Ecography *44*, 1808–1811. https://doi.org/10.1111/ecog.05895.

30. Ledger, S.E.H., Loh, J., Almond, R., Böhm, M., Clements, C.F., Currie, J., Deinet, S., Galewski, T., Grooten, M., Jenkins, M., et al. (2023). Past, present, and future of the Living Planet Index. Npj Biodivers. *2*, 12. https://doi.org/10.1038/s44185-023-00017-3.

31. Adamowicz, S.J., and Steinke, D. (2015). Increasing global participation in genetics research through DNA barcoding. Genome *58*, 519–526. https://doi.org/10.1139/gen-2015-0130.

32. Faith, D.P. (1992). Conservation evaluation and phylogenetic diversity. Biol. Conserv. *61*, 1–10. https://doi.org/10.1016/0006-3207(92)91201-3.

33. Graham, C.H., and Hijmans, R.J. (2006). A comparison of methods for mapping species ranges and species richness. Glob. Ecol. Biogeogr. *15*, 578–587. https://doi.org/10.1111/j.1466-8238.2006.00257.x.

34. Jenkins, C.N., Pimm, S.L., and Joppa, L.N. (2013). Global patterns of terrestrial vertebrate diversity and conservation. Proc. Natl. Acad. Sci. *110*, E2602–E2610. https://doi.org/10.1073/pnas.1302251110.

35. Roll, U., Feldman, A., Novosolov, M., Allison, A., Bauer, A.M., Bernard, R., Böhm, M., Castro-Herrera, F., Chirio, L., Collen, B., et al. (2017). The global distribution of tetrapods reveals a need for targeted reptile conservation. Nat. Ecol. Evol. *1*, 1677–1682. https://doi.org/10.1038/s41559-017-0332-2.

36. Cai, L., Kreft, H., Taylor, A., Denelle, P., Schrader, J., Essl, F., van Kleunen, M., Pergl, J., Pyšek, P., Stein, A., et al. (2023). Global models and predictions of plant diversity based on advanced machine learning techniques. New Phytol. *237*, 1432–1445. https://doi.org/10.1111/nph.18533.

37. Ellis, E.C., Antill, E.C., and Kreft, H. (2012). All Is Not Loss: Plant Biodiversity in the Anthropocene. PLOS ONE *7*, e30535. https://doi.org/10.1371/journal.pone.0030535.

38. Kreft, H., and Jetz, W. (2007). Global patterns and determinants of vascular plant diversity. Proc. Natl. Acad. Sci. *104*, 5925–5930. https://doi.org/10.1073/pnas.0608361104.

39. Fritz, S.A., and Rahbek, C. (2012). Global patterns of amphibian phylogenetic diversity. J. Biogeogr. *39*, 1373–1382. https://doi.org/10.1111/j.1365-2699.2012.02757.x.

40. Wolf, S., Mahecha, M.D., Sabatini, F.M., Wirth, C., Bruelheide, H., Kattge, J., Moreno Martínez, Á., Mora, K., and Kattenborn, T. (2022). Citizen science plant observations encode global trait patterns. Nat. Ecol. Evol. *6*, 1850–1859. https://doi.org/10.1038/s41559-022-01904-x.

41. Rodrigues, A.S.L., Pilgrim, J.D., Lamoreux, J.F., Hoffmann, M., and Brooks, T.M. (2006). The value of the IUCN Red List for conservation. Trends Ecol. Evol. *21*, 71–76. https://doi.org/10.1016/j.tree.2005.10.010.

42. Howard, C., Flather, C.H., and Stephens, P.A. (2020). A global assessment of the drivers of threatened terrestrial species richness. Nat. Commun. *11*, 993. https://doi.org/10.1038/s41467-020-14771-6.

43. Hughes, A.C., Orr, M.C., Yang, Q., and Qiao, H. (2021). Effectively and accurately mapping global biodiversity patterns for different regions and taxa. Glob. Ecol. Biogeogr. *30*, 1375–1388. https://doi.org/10.1111/geb.13304.

44. Jung, M., Arnell, A., de Lamo, X., García-Rangel, S., Lewis, M., Mark, J., Merow, C., Miles, L., Ondo, I., Pironon, S., et al. (2021). Areas of global importance for conserving terrestrial

biodiversity, carbon and water. Nat. Ecol. Evol. *5*, 1499–1509. https://doi.org/10.1038/s41559-021-01528-7.

45. Mueller, G.M., Cunha, K.M., May, T.W., Allen, J.L., Westrip, J.R.S., Canteiro, C., Costa-Rezende, D.H., Drechsler-Santos, E.R., Vasco-Palacios, A.M., Ainsworth, A.M., et al. (2022). What Do the First 597 Global Fungal Red List Assessments Tell Us about the Threat Status of Fungi? Diversity *14*, 736. https://doi.org/10.3390/d14090736.

46. Locey, K.J., and Lennon, J.T. (2016). Scaling laws predict global microbial diversity. Proc. Natl. Acad. Sci. *113*, 5970–5975. https://doi.org/10.1073/pnas.1521291113.

47. Larsen, B.B., Miller, E.C., Rhodes, M.K., and Wiens, J.J. (2017). Inordinate Fondness Multiplied and Redistributed: the Number of Species on Earth and the New Pie of Life. Q. Rev. Biol. *92*, 229–265. https://doi.org/10.1086/693564.

48. Ruppert, K.M., Kline, R.J., and Rahman, M.S. (2019). Past, present, and future perspectives of environmental DNA (eDNA) metabarcoding: A systematic review in methods, monitoring, and applications of global eDNA. Glob. Ecol. Conserv. *17*, e00547. https://doi.org/10.1016/j.gecco.2019.e00547.

49. Větrovský, T., Morais, D., Kohout, P., Lepinay, C., Algora, C., Awokunle Hollá, S., Bahnmann, B.D., Bílohnědá, K., Brabcová, V., D’Alò, F., et al. (2020). GlobalFungi, a global database of fungal occurrences from high-throughput-sequencing metabarcoding studies. Sci. Data *7*, 228. https://doi.org/10.1038/s41597-020-0567-7.

50. Mikryukov, V., Dulya, O., Zizka, A., Bahram, M., Hagh-Doust, N., Anslan, S., Prylutskyi, O., Delgado-Baquerizo, M., Maestre, F.T., Nilsson, H., et al. (2023). Connecting the multiple dimensions of global soil fungal diversity. Sci. Adv. *9*, eadj8016. https://doi.org/10.1126/sciadv.adj8016.

51. Li, P., Tedersoo, L., Crowther, T.W., Wang, B., Shi, Y., Kuang, L., Li, T., Wu, M., Liu, M., Luan, L., et al. (2023). Global diversity and biogeography of potential phytopathogenic fungi in a changing world. Nat. Commun. *14*, 6482. https://doi.org/10.1038/s41467-023-42142-4.

52. Delgado-Baquerizo, M., Oliverio, A.M., Brewer, T.E., Benavent-González, A., Eldridge, D.J., Bardgett, R.D., Maestre, F.T., Singh, B.K., and Fierer, N. (2018). A global atlas of the dominant bacteria found in soil. Science *359*, 320–325. https://doi.org/10.1126/science.aap9516.

53. Sanderson, E.W., Jaiteh, M., Levy, M.A., Redford, K.H., Wannebo, A.V., and Woolmer, G. (2002). The Human Footprint and the Last of the Wild. BioScience *52*, 891. https://doi.org/10.1641/0006-3568(2002)052[0891:THFATL]2.0.CO;2.

54. Venter, O., Sanderson, E.W., Magrach, A., Allan, J.R., Beher, J., Jones, K.R., Possingham, H.P., Laurance, W.F., Wood, P., Fekete, B.M., et al. (2016). Global terrestrial Human Footprint maps for 1993 and 2009. Sci. Data *3*, 160067. https://doi.org/10.1038/sdata.2016.67.

55. Kennedy, C.M., Oakleaf, J.R., Theobald, D.M., Baruch-Mordo, S., and Kiesecker, J. (2019). Managing the middle: A shift in conservation priorities based on the global human modification gradient. Glob. Change Biol. *25*, 811–826. https://doi.org/10.1111/gcb.14549.

56. Theobald, D.M., Kennedy, C., Chen, B., Oakleaf, J., Baruch-Mordo, S., and Kiesecker, J. (2020). Earth transformed: detailed mapping of global human modification from 1990 to 2017. Earth Syst. Sci. Data *12*, 1953–1972. https://doi.org/10.5194/essd-12-1953-2020.

57. Jung, M., Dahal, P.R., Butchart, S.H.M., Donald, P.F., De Lamo, X., Lesiv, M., Kapos, V., Rondinini, C., and Visconti, P. (2020). A global map of terrestrial habitat types. Sci. Data *7*, 256. https://doi.org/10.1038/s41597-020-00599-8.

58. Hansen, M.C., Potapov, P.V., Moore, R., Hancher, M., Turubanova, S.A., Tyukavina, A., Thau, D., Stehman, S.V., Goetz, S.J., Loveland, T.R., et al. (2013). High-Resolution Global Maps of 21st-Century Forest Cover Change. Science *342*, 850–853. https://doi.org/10.1126/science.1244693.

59. Lang, N., Jetz, W., Schindler, K., and Wegner, J.D. (2023). A high-resolution canopy height model of the Earth. Nat. Ecol. Evol. *7*, 1778–1789. https://doi.org/10.1038/s41559-023-02206-6.

60. Spawn, S.A., Sullivan, C.C., Lark, T.J., and Gibbs, H.K. (2020). Harmonized global maps of above and belowground biomass carbon density in the year 2010. Sci. Data *7*, 112. https://doi.org/10.1038/s41597-020-0444-4.

61. Ma, H., Mo, L., Crowther, T.W., Maynard, D.S., Van Den Hoogen, J., Stocker, B.D., Terrer, C., and Zohner, C.M. (2021). The global distribution and environmental drivers of aboveground versus belowground plant biomass. Nat. Ecol. Evol. *5*, 1110–1122. https://doi.org/10.1038/s41559-021-01485-1.

62. Warner, D.L., Bond-Lamberty, B.P., Jian, J., Stell, E., and Vargas, R. (2019). Carbon Monitoring System (CMS)Global Gridded 1-km Annual Soil Respiration and Uncertainty Derived from SRDB V3. Preprint at ORNL Distributed Active Archive Center, https://doi.org/10.3334/ORNLDAAC/1736 https://doi.org/10.3334/ORNLDAAC/1736.

63. Tuanmu, M.-N., and Jetz, W. (2015). A global, remote sensing-based characterization of terrestrial habitat heterogeneity for biodiversity and ecosystem modelling. Glob. Ecol. Biogeogr. *24*, 1329–1339. https://doi.org/10.1111/geb.12365.

64. Myneni, R., Knyazikhin, Y., and Park, T. (2021). MODIS/Terra+Aqua Leaf Area Index/FPAR 4-Day L4 Global 500m SIN Grid V061. (NASA EOSDIS Land Processes Distributed Active Archive Center). https://doi.org/10.5067/MODIS/MCD15A3H.061 https://doi.org/10.5067/MODIS/MCD15A3H.061.

65. Cisneros-Araujo, P., Goicolea, T., Mateo-Sánchez, M.C., García-Viñás, J.I., Marchamalo, M., Mercier, A., and Gastón, A. (2021). The Role of Remote Sensing Data in Habitat Suitability

and Connectivity Modeling: Insights from the Cantabrian Brown Bear. Remote Sens. *13*, 1138. https://doi.org/10.3390/rs13061138.

66. Cisneros-Araujo, P., Ramirez-Lopez, M., Juffe-Bignoli, D., Fensholt, R., Muro, J., Mateo-Sánchez, M.C., and Burgess, N.D. (2021). Remote sensing of wildlife connectivity networks and priority locations for conservation in the Southern Agricultural Growth Corridor (SAGCOT) in Tanzania. Remote Sens. Ecol. Conserv. *7*, 430–444. https://doi.org/10.1002/rse2.199.

67. Running, S.W., and Zhao, M. Daily GPP and Annual NPP (MOD17A2/A3) Products NASA Earth Observing System MODIS Land Algorithm.

68. Smith, T., Traxl, D., and Boers, N. (2022). Empirical evidence for recent global shifts in vegetation resilience. Nat. Clim. Change *12*, 477–484. https://doi.org/10.1038/s41558-022-01352-2.

69. Seddon, A.W.R., Macias-Fauria, M., Long, P.R., Benz, D., and Willis, K.J. (2016). Sensitivity of global terrestrial ecosystems to climate variability. Nature *531*, 229–232. https://doi.org/10.1038/nature16986.

70. Giri, C., Ochieng, E., Tieszen, L.L., Zhu, Z., Singh, A., Loveland, T., Masek, J., and Duke, N. (2011). Status and distribution of mangrove forests of the world using earth observation satellite data. Glob. Ecol. Biogeogr. *20*, 154–159. https://doi.org/10.1111/j.1466-8238.2010.00584.x.

71. Xu, J., Morris, P.J., Liu, J., and Holden, J. (2018). PEATMAP: Refining estimates of global peatland distribution based on a meta-analysis. CATENA *160*, 134–140. https://doi.org/10.1016/j.catena.2017.09.010.

72. T., G., R.M., R.-C., L.V., V., M., H., F., W., E., H., N., H., and D., M. Tropical and Subtropical Wetlands Distribution version 2. https://doi.org/10.17528/cifor/data.00058 https://doi.org/10.17528/cifor/data.00058.

73. Mendes, S.B., Olesen, J.M., Memmott, J., Costa, J.M., Timóteo, S., Dengucho, A.L., Craveiro, L., and Heleno, R. (2024). Evidence of a European seed dispersal crisis. Science *386*, 206–211. https://doi.org/10.1126/science.ado1464.

74. GFBI consortium, Steidinger, B.S., Crowther, T.W., Liang, J., Van Nuland, M.E., Werner, G.D.A., Reich, P.B., Nabuurs, G.J., de-Miguel, S., Zhou, M., et al. (2019). Climatic controls of decomposition drive the global biogeography of forest-tree symbioses. Nature *569*, 404–408. https://doi.org/10.1038/s41586-019-1128-0.

75. Barceló, M., Van Bodegom, P.M., and Soudzilovskaia, N.A. (2023). Fine-resolution global maps of root biomass carbon colonized by arbuscular and ectomycorrhizal fungi. Sci. Data *10*, 56. https://doi.org/10.1038/s41597-022-01913-2.

76. Rodell, M., Houser, P.R., Jambor, U., Gottschalck, J., Mitchell, K., Meng, C.-J., Arsenault, K., Cosgrove, B., Radakovich, J., Bosilovich, M., et al. (2004). The Global Land Data Assimilation System. Bull. Am. Meteorol. Soc. *85*, 381–394. https://doi.org/10.1175/BAMS-85-3-381.

77. Tuomi, M., Laiho, R., Repo, A., and Liski, J. (2011). Wood decomposition model for boreal forests. Ecol. Model. *222*, 709–718. https://doi.org/10.1016/j.ecolmodel.2010.10.025.

78. Assis, J.C., Hohlenwerger, C., Metzger, J.P., Rhodes, J.R., Duarte, G.T., da Silva, R.A., Boesing, A.L., Prist, P.R., and Ribeiro, M.C. (2023). Linking landscape structure and ecosystem service flow. Ecosyst. Serv. *62*, 101535. https://doi.org/10.1016/j.ecoser.2023.101535.

79. Baude, M., and Meyer, B.C. (2023). Changes in landscape structure and ecosystem services since 1850 analyzed using landscape metrics in two German municipalities. Ecol. Indic. *152*, 110365. https://doi.org/10.1016/j.ecolind.2023.110365.

80. Belote, R.T., Barnett, K., Zeller, K., Brennan, A., and Gage, J. (2022). Examining local and regional ecological connectivity throughout North America. Landsc. Ecol. *37*, 2977–2990. https://doi.org/10.1007/s10980-022-01530-9.

81. Beyer, H.L., Venter, O., Grantham, H.S., and Watson, J.E.M. (2020). Substantial losses in ecoregion intactness highlight urgency of globally coordinated action. Conserv. Lett. *13*, e12692. https://doi.org/10.1111/conl.12692.

82. Liu, S., Dong, Y., Deng, L., Liu, Q., Zhao, H., and Dong, S. (2014). Forest fragmentation and landscape connectivity change associated with road network extension and city expansion: A case study in the Lancang River Valley. Ecol. Indic. *36*, 160–168. https://doi.org/10.1016/j.ecolind.2013.07.018.

83. Hill, S.L.L., Fajardo, J., Maney, C., Harfoot, M., Harrison, M., Guaras, D., Jones, M., Oliva, M.J., Danks, F., Hughes, J., et al. (2022). The Ecosystem Integrity Index: a novel measure of terrestrial ecosystem integrity with global coverage (Ecology) https://doi.org/10.1101/2022.08.21.504707.

84. Newbold, T., Hudson, L.N., Arnell, A.P., Contu, S., De Palma, A., Ferrier, S., Hill, S.L.L., Hoskins, A.J., Lysenko, I., Phillips, H.R.P., et al. (2016). Has land use pushed terrestrial biodiversity beyond the planetary boundary? A global assessment. Science *353*, 288–291. https://doi.org/10.1126/science.aaf2201.

85. De Palma, A., Hoskins, A., Gonzalez, R.E., Börger, L., Newbold, T., Sanchez-Ortiz, K., Ferrier, S., and Purvis, A. (2021). Annual changes in the Biodiversity Intactness Index in tropical and subtropical forest biomes, 2001–2012. Sci. Rep. *11*, 20249. https://doi.org/10.1038/s41598-021-98811-1.

86. Schipper, A.M., Hilbers, J.P., Meijer, J.R., Antão, L.H., Benítez-López, A., de Jonge, M.M.J., Leemans, L.H., Scheper, E., Alkemade, R., Doelman, J.C., et al. (2020). Projecting terrestrial biodiversity intactness with GLOBIO 4. Glob. Change Biol. *26*, 760–771. https://doi.org/10.1111/gcb.14848.

87. Hill, S.L.L., Gonzalez, R., Sanchez-Ortiz, K., Caton, E., Espinoza, F., Newbold, T., Tylianakis, J., Scharlemann, J.P.W., De Palma, A., and Purvis, A. (2018). Worldwide impacts of past and projected future land-use change on local species richness and the Biodiversity Intactness Index (Ecology) https://doi.org/10.1101/311787.

88. Hudson, L.N., Newbold, T., Contu, S., Hill, S.L.L., Lysenko, I., De Palma, A., Phillips, H.R.P., Senior, R.A., Bennett, D.J., Booth, H., et al. (2014). The PREDICTS database: a global database of how local terrestrial biodiversity responds to human impacts. Ecol. Evol. *4*, 4701–4735. https://doi.org/10.1002/ece3.1303.

89. Hudson, L.N., Newbold, T., Contu, S., Hill, S.L.L., Lysenko, I., De Palma, A., Phillips, H.R.P., Alhusseini, T.I., Bedford, F.E., Bennett, D.J., et al. (2017). The database of the PREDICTS (Projecting Responses of Ecological Diversity In Changing Terrestrial Systems) project. Ecol. Evol. *7*, 145–188. https://doi.org/10.1002/ece3.2579.

90. Liu, L., Zhu, K., Wurzburger, N., and Zhang, J. (2020). Relationships between plant diversity and soil microbial diversity vary across taxonomic groups and spatial scales. Ecosphere *11*, e02999. https://doi.org/10.1002/ecs2.2999.

91. Prober, S.M., Leff, J.W., Bates, S.T., Borer, E.T., Firn, J., Harpole, W.S., Lind, E.M., Seabloom, E.W., Adler, P.B., Bakker, J.D., et al. (2015). Plant diversity predicts beta but not alpha diversity of soil microbes across grasslands worldwide. Ecol. Lett. *18*, 85–95. https://doi.org/10.1111/ele.12381.

92. Kwok, R. (2018). Ecology's remote-sensing revolution. Nature *556*, 137–138. https://doi.org/10.1038/d41586-018-03924-9.

93. Farley, S.S., Dawson, A., Goring, S.J., and Williams, J.W. (2018). Situating Ecology as a Big-Data Science: Current Advances, Challenges, and Solutions. BioScience *68*, 563–576. https://doi.org/10.1093/biosci/biy068.

94. Abe, S. (2005). Training of Support Vector Machines with Mahalanobis Kernels. In Artificial Neural Networks: Formal Models and Their Applications – ICANN 2005 Lecture Notes in Computer Science., W. Duch, J. Kacprzyk, E. Oja, and S. Zadrożny, eds. (Springer Berlin Heidelberg), pp. 571–576. https://doi.org/10.1007/11550907_90.

95. Gallagher, R., and Carpenter, B. (1997). Human-Dominated Ecosystems. Science *277*, 485–485. https://doi.org/10.1126/science.277.5325.485.

96. Balaguer, L., Escudero, A., Martín-Duque, J.F., Mola, I., and Aronson, J. (2014). The historical reference in restoration ecology: Re-defining a cornerstone concept. Biol. Conserv. *176*, 12–20. https://doi.org/10.1016/j.biocon.2014.05.007.

97. Dinerstein, E., Olson, D., Joshi, A., Vynne, C., Burgess, N.D., Wikramanayake, E., Hahn, N., Palminteri, S., Hedao, P., Noss, R., et al. (2017). An Ecoregion-Based Approach to Protecting Half the Terrestrial Realm. BioScience *67*, 534–545. https://doi.org/10.1093/biosci/bix014.

98. Suding, K.N. (2011). Toward an Era of Restoration in Ecology: Successes, Failures, and Opportunities Ahead. Annu. Rev. Ecol. Evol. Syst. *42*, 465–487. https://doi.org/10.1146/annurev-ecolsys-102710-145115.

99. Runfola, D., Anderson, A., Baier, H., Crittenden, M., Dowker, E., Fuhrig, S., Goodman, S., Grimsley, G., Layko, R., Melville, G., et al. (2020). geoBoundaries: A global database of political administrative boundaries. PLOS ONE *15*, e0231866. https://doi.org/10.1371/journal.pone.0231866.

100. Jetz, W., McPherson, J.M., and Guralnick, R.P. (2012). Integrating biodiversity distribution knowledge: toward a global map of life. Trends Ecol. Evol. *27*, 151–159. https://doi.org/10.1016/j.tree.2011.09.007.

101. Paz, A., Silva, T.S., and Carnaval, A.C. (2022). A framework for near-real time monitoring of diversity patterns based on indirect remote sensing, with an application in the Brazilian Atlantic rainforest. PeerJ *10*, e13534. https://doi.org/10.7717/peerj.13534.

102. Turner, W. (2014). Sensing biodiversity. Science *346*, 301–302. https://doi.org/10.1126/science.1256014.

103. Cawse-Nicholson, K., Townsend, P.A., Schimel, D., Assiri, A.M., Blake, P.L., Buongiorno, M.F., Campbell, P., Carmon, N., Casey, K.A., Correa-Pabón, R.E., et al. (2021). NASA's surface biology and geology designated observable: A perspective on surface imaging algorithms. Remote Sens. Environ. *257*, 112349. https://doi.org/10.1016/j.rse.2021.112349.

104. European Space Agency (2020). Chime (Copernicus Hyperspectral Imaging Mission for the Environment) - eoPortal. https://www.eoportal.org/satellite-missions/chime-copernicus#eop-quick-facts-section.

105. Cavender-Bares, J., Gamon, J.A., Hobbie, S.E., Madritch, M.D., Meireles, J.E., Schweiger, A.K., and Townsend, P.A. (2017). Harnessing plant spectra to integrate the biodiversity sciences across biological and spatial scales. Am. J. Bot. *104*, 966–969. https://doi.org/10.3732/ajb.1700061.

106. Deiner, K., Bik, H.M., Mächler, E., Seymour, M., Lacoursière-Roussel, A., Altermatt, F., Creer, S., Bista, I., Lodge, D.M., de Vere, N., et al. (2017). Environmental DNA metabarcoding: Transforming how we survey animal and plant communities. Mol. Ecol. *26*, 5872–5895. https://doi.org/10.1111/mec.14350.

107. Sueur, J., and Farina, A. (2015). Ecoacoustics: the Ecological Investigation and Interpretation of Environmental Sound. Biosemiotics *8*, 493–502. https://doi.org/10.1007/s12304-015-9248-x.

108. Buřivalová, Z., Yoh, N., Butler, R.A., Chandra Sagar, H.S.S., and Game, E.T. (2023). Broadening the focus of forest conservation beyond carbon. Curr. Biol. *33*, R621–R635. https://doi.org/10.1016/j.cub.2023.04.019.

109. Dasgupta, P. (2021). The Economics of Biodiversity: The Dasgupta Review.

110. The Bonn Challenge | Bonchallenge https://www.bonnchallenge.org/.

111. THE 17 GOALS | Sustainable Development https://sdgs.un.org/goals.

112. Science Based Targets Network Sci. Based Targets Netw. https://sciencebasedtargetsnetwork.org/.

113. European Space Agency (2022). Copernicus Sentinel-2 (processed by ESA), 2022, MSI Level-2A BOA Reflectance Product. Collection 1.

114. Sabatini, F.M., Jiménez-Alfaro, B., Jandt, U., Chytrý, M., Field, R., Kessler, M., Lenoir, J., Schrodt, F., Wiser, S.K., Arfin Khan, M.A.S., et al. (2022). Global patterns of vascular plant alpha diversity. Nat. Commun. *13,* 4683. https://doi.org/10.1038/s41467-022-32063-z.

115. Sanchez-Ortiz, K., Gonzalez, R.E., De Palma, A., Newbold, T., Hill, S.L.L., Tylianakis, J.M., Börger, L., Lysenko, I., and Purvis, A. (2019). Land-use and related pressures have reduced biotic integrity more on islands than on mainlands. Preprint, https://doi.org/10.1101/576546 https://doi.org/10.1101/576546.

116. Impact Observatory and Vizzuality Biodiversity Intactness Index (BII). (Google Earth Engine:projects/ebx-data/assets/earthblox/IO/BIOINTACT).

Supplement S1

Reference Area Methodology

We developed an approach that offers a contemporary baseline which all global biodiversity maps may be evaluated. Our algorithm uses the human modification index (HMI)[55] and potential natural vegetation (PNV)[57] to create a reference area mask that delineates the relatively pristine areas on the globe. The combination of PNV classes and 846 delineated ecoregions[97] then guides the assignment of reference areas to all non-reference pixels having the same ecoregion-PNV class. Due to the large variations in the extent of human modification among different ecoregion landcover combinations, we designed a dynamic decision tree for selecting a threshold HMI to define reference pixels and then to link reference to non-reference pixels to obtain the reference mask.

We targeted reference pixels with minimal human modification which we defined as follows. For each PNV class, v, within each ecoregion, e, we calculated the 5th and 3rd percentile of the HMI, $P_{0.05}(HMI_{e,v})$ and $P_{0.03}(HMI_{e,v})$. The reference threshold value, $r_{e,v}$ was then set to the maximum of either $P_{0.05}(HMI_{e,v})$ or $P_{0.03}(HMI_{e,v})$ if they were less than 0.05, or 0.05 (See equation S1 below).

$$r_{e,v} = \begin{cases} P_{0.05}(HMI_{e,v}) & if\ P_{0.05}(HMI_{e,v}) \leq 0.05 \\ P_{0.03}(HMI_{e,v}) & if\ P_{0.05}(HMI_{e,v}) > 0.05\ and\ P_{0.03}(HMI_{e,v}) \leq 0.05 \\ 0.05 & if\ P_{0.05}(HMI_{e,v}) > 0.05\ and\ P_{0.03}(HMI_{e,v}) > 0.05 \end{cases} \qquad \text{Equation S1}$$

We set these criteria to focus the reference areas in relative unmodified ecoregions, while allowing a more inclusion in reference where needed, but only to the point of an HMI equal to 0.05. With the threshold defined for each ecoregion-PNV class, we selected reference areas as all pixels less than $r_{e,v}$. If an ecoregion-PNV class had fewer than five pixels, we stepped down the reference threshold – from the $P_{0.05}(HMI_{e,v})$ to $P_{0.03}(HMI_{e,v})$, or from $P_{0.03}(HMI_{e,v})$ to $0.05(x_{e,v}, y_{e,v})$. If $r_{e,v}$ was 0.05, and the ecoregion-PNV class still possessed fewer than five reference pixels, then we looked beyond the ecoregion boundary and included all reference pixels of the same PNV class within the same biome.

Delta calculation

To calculate the delta value for each axis of the seed index, we use the following formula:

$$K = e^{-\delta D}$$

where K is the kernel, δ is the delta parameter and D is the maximum Manhattan distance of the axis for all the pixel points. This effectively maps the highest possible distance of the layers of the axis to the lowest kernel value of the axis possible. In this case we define this lowest kernel value as 0.001. By solving for δ parameter as other values in the equation are known we can get the delta value for each of the axis. We then substitute this delta value in the equation to calculate the kernel for the world of each axis. The SEED index is then calculated based on the weighted average of the individual axes.

Table S1. Table of scores, weights, and a description of the criteria guiding our judgment in rating the quality of information contained with each map that we incorporated in SEED.

Confidence Score	Weight	Description
5	100	Fully validated model representing on the ground conditions with at least 1-km resolution
4	90	Partially validated model representing on the ground conditions with at least 1-km resolution
3	50	Model predicting on the ground conditions with at least 5-km resolution, requires validation
2	10	Model predicting general diversity patterns with some human impacts considered
1	1	Model of general diversity patterns. Does not represent human impacts on nature.

To compare SEED with three of the most commonly used global indices, we computed the difference between SEED and the MSA from GLOBIO[86], the BII from the Natural History Museum[115], and a second BII (which we will call BDI) produced with a less recent version of the same core methodology[84,116]. The broad scale differences in our index indicate that SEED may be more conservative than MSA and BII (Figure S1a-b) in boreal and desert regions, while SEED estimates higher intactness across temperate regions, sub-Saharan Africa, South Africa, and parts of Australia (Figure S1a-b). SEED was consistently lower than the BDI globally (Figure S1c). Underlying these differences, the distribution of MSA and BII values are bimodal compared with the BDI and SEED, which are unimodal. This means that MSA and BII may more commonly characterize an ecosystem as either highly intact or not very intact, while SEED would more commonly characterize the same ecosystem as moderately intact.

a) Mean Species Abundance (GLOBIO)

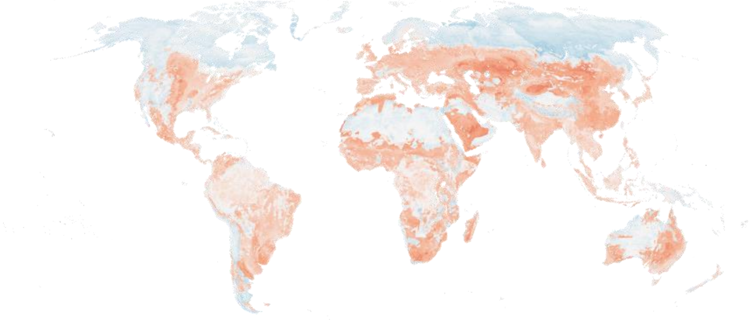

b) Biodiversity Intactness Index (Natural History Museum)

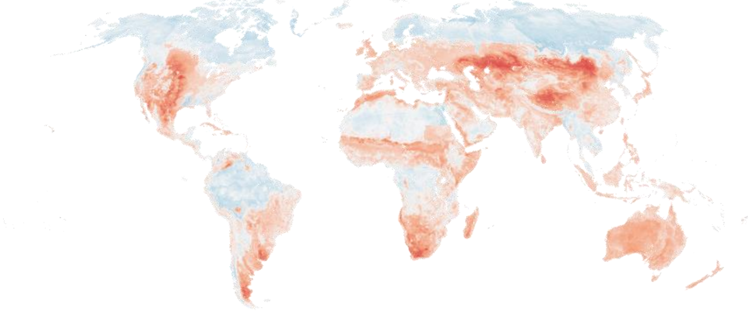

c) Biodiversity Intactness Index (Impact Observatory and Vizzuality)

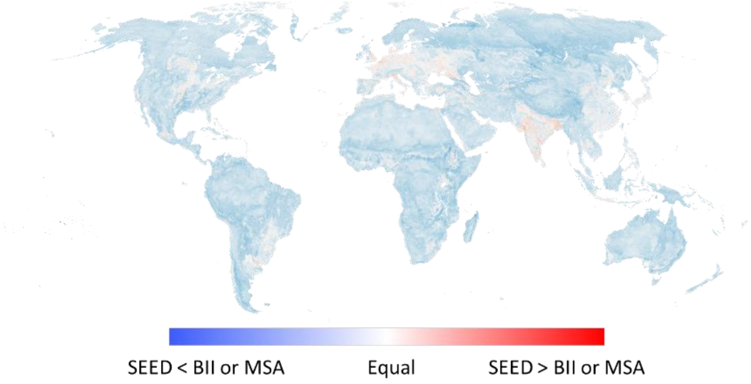

Figure S1. Comparison with leading global biodiversity models. Global showing the difference between SEED and (a) MSA[86], (b) BII from NHM[115], and (c) BDI, which was created independently from the BII while using the same model[116].